

Morphological Characteristics of Shrub Coppice Dunes in Desert Grasslands of Southern New Mexico derived from Scanning LIDAR

A. Rango,* M. Chopping,* J. Ritchie,* K. Havstad,† W. Kustas*
and T. Schmugge*

Since the 1880s rangeland vegetation in southern New Mexico has changed dramatically over widespread areas, typically with shrublands displacing native grasslands. Coincident with these changes in vegetation dominance are increases in soil erosion, stream channel cutting, and shrub coppice dune formation on sandy soils. Where marked transitions in vegetation type from grassland to honey mesquite shrubland have occurred, the local topography has been transformed with previously flat mesa becoming rolling duneland. The size, distribution, and morphological characteristics of these dunes have an important impact on fluxes of energy and nutrients at the surface; they also render the land far less useful as grazing land for domestic livestock. These shrub coppice dunes and the mesquite shrubs that grow on them may be considered roughness elements. Quantifying their morphology is important for the calculation of aerodynamic roughness length and displacement height. This article tests the ability of active scanning laser remote sensing techniques to provide accurate estimates of the three-dimensional shapes and areal distributions of dune and interdune areas. It shows that scanning laser with a

footprint diameter of 0.38 m and a sampling interval of 1.5 m to 2 m can be used to measure the morphological characteristics of shrub coppice dunes in the desert grasslands of southern New Mexico with acceptable accuracy and precision for a range of uses, including important geomorphological and hydrological applications. The use of scanning laser systems together with optical multi-spectral data is shown to be highly synergistic, providing information that is not easily obtainable via other surveying methods. ©Elsevier Science Inc., 2000

INTRODUCTION

Global climate change has become a prominent concern in the arid and semiarid portions of the southwestern United States. Since these arid and semiarid regions are very sensitive to climate variations, much work has been devoted to identifying changing rangeland vegetation patterns and attempting to link these changes to possible causes. Since the 1880s, rangeland vegetation has changed significantly in widespread areas, typically with shrubs displacing valuable native grasses. This change has been extensively documented by field measurement (Buffington and Herbel, 1965). The change in vegetation has further been documented by comparisons of historical and current photographs (rephotography) (Hastings and Turner, 1965; Bahre, 1991; Webb, 1996). Melton (1940) indicated that these mesquite-coppice dunes were present in vast numbers in southeastern New Mexico by the 1940s.

One of the key factors causing the change was extreme overstocking of the arid and semiarid rangelands with cattle and sheep in the 1880s (Smith, 1899; Wooton, 1908).

Trade names are included for the benefit of the reader and do not imply an endorsement of or a preference for the product listed by the U.S. Department of Agriculture.

* USDA ARS Hydrology Laboratory, BARC-W, Beltsville, MD 20705

† USDA ARS Jornada Experimental Range, Las Cruces, NM 88003

Address correspondence to Dr. Albert Rango, USDA ARS Hydrology Laboratory, Rm 104, Bldg. 007 BARC-West, Beltsville, MD 20705, USA. E-mail: alrango@hydrolab.arsusda.gov

Received 27 September 1999; revised 6 January 2000.

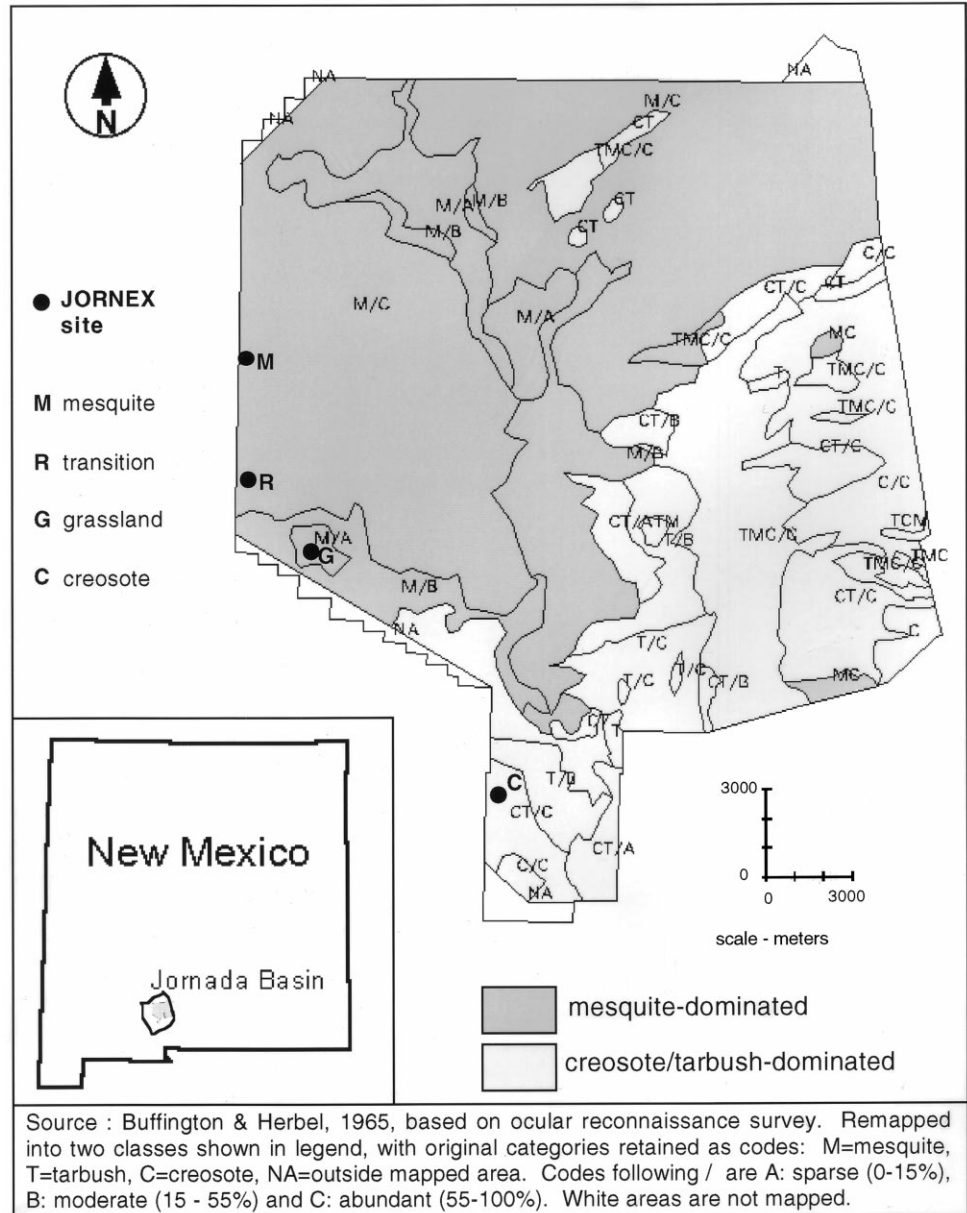


Figure 1. Location of the JORNEX study sites and the USDA-ARS Jornada Experimental Range.

In 1870, approximately 0.7 million head of livestock were grazing in New Mexico but numbers increased to about 5.8 million head by 1885 (0.8 million cattle and 5 million sheep) (Fredrickson et al., 1997). Drought years in the late 1880s and early 1890s put severe stress on grazing land vegetation (Grover and Musick, 1990). Native grass cover was reduced so much by the extreme overgrazing and drought that shrubs such as creosote bush (*Larrea spp.*) and mesquite (*Prosopis spp.*) invaded grasslands. For many areas the vegetation change was relatively quick and the shrubs were not easily displaced. This invasion by mesquite has been described as a two-stage process of dispersal and establishment (Archer et al., 1988; Archer, 1989; Archer, 1994). Records from the Jornada Experimental Range near Las Cruces, New Mexico

(Fig. 1) illustrate these vegetation dynamics. In the area covered by vegetation surveys (585 km²) 388 km² or 58% was native grassland with no shrubs (mesquite, tarbrush, or creosote bush) (Buffington and Herbel, 1965) in 1858. By 1915 native grassland areas had been reduced to 144 km² or 25%; by 1928 the grassland had been further reduced to 133 km² or 23%; and by 1963 there was no native grassland totally free of shrubs. Experiments to try to stop the growth of mesquite and to reestablish grass cover were carried out at the Jornada Experimental Range in the 1930s. These included controls on rodent populations, cutting back of mesquite root systems, and planting and seeding of various grasses. None of these techniques were found to be wholly successful in arresting the mesquite growth and reestablishing grass cover



Figure 2. Photograph of the JORNEX mesquite coppice dune site, USDA-ARS Jornada Experimental Range.

(Valentine, 1942). Coincident with this change in vegetation dominance were increases in soil erosion, stream channel cutting, and coppice dune formation on sandy soils.

In recognition that rangelands make up the largest single land use in the United States (about 50% of the total land area) and that sustainable management of these areas will require assessment of rangeland conditions over large areas, the *JORNada EXperiment* (JORNEX) was initiated in 1995 (Rango et al., 1998). JORNEX has several overarching objectives including: (a) the development of remote sensing methods to assess rangeland condition, (b) quantification of various characteristics of rangeland vegetation, and (c) measurement of plant/atmosphere interactions for use in evaluating global change effects. Numerous techniques for monitoring rangeland condition and change have been and are being developed (Ritchie et al., 1996). One of the areas on the Jornada Experimental Range that shows evidence of dramatic landscape change is the area dominated by mesquite coppice sand dunes (Fig. 2). This area is distinguished from native grasslands by a marked difference in vegetation type (grass to shrub) and local topography (flat mesa to rolling duneland). Quantification of the characteristics of the mesquite coppice sand dunes has been addressed using airborne remote sensing with visible and thermal infrared imagery, multispectral video digital imagery, photog-

raphy, and laser altimetry (Ritchie, 1995; Ritchie et al., 1996; Everitt et al., 1997; Pachepsky and Ritchie, 1998; Rango et al., 1998). Ground-based techniques have included thermal measurements, leaf area index measurements, vegetation line transect surveys, surface energy flux measurements, and engineering field surveying to measure elevation differences (Rango et al., 1998). The objective of the present study was to characterize the areal and vertical variability of the coppice dunes, interdunes, and mesquite dune vegetation based on novel airborne remote sensing techniques with validation provided by ground measurements.

BACKGROUND

Much literature exists dealing with the degradation of native grasslands through the replacement of perennial grasses by mesquite and other shrubs (Schlesinger et al., 1990; Huenneke, 1996). The information on associated building of coppice dunes is more limited. For coppice dunes to form, a vegetation type that tolerates having its roots and branches buried by sand is required. In the southwestern United States that species is usually honey mesquite (*Prosopis glandulosa*); creosote bush, for example, will not flourish under these conditions (Gay and Dwyer, 1998). Other shrubs that will occur and dominate on dune landscapes are sand sage, broom dalea, *Grayia*

spinosa (Link et al., 1994), Wyoming big sagebrush (Blackburn et al., 1990), and blackbrush (Blackburn and Wood, 1990) and four wing saltbush (*Atriplex canescens*). The tolerant shrub serves as a lattice to catch the sand, causing a vertical buildup; the shrub thus continues to grow and spread over the dune top. Two additional factors are necessary: wind movement to transport the sands and sandy soils to supply the transported material. Studies in rangelands of the western United States (Belnap and Gillette, 1997) and the Jornada Experimental Range in particular (Marticorena et al., 1997) show that the threshold wind friction velocity for loose sandy soil ranges from 15 to 50 cm sec⁻¹. This wind speed threshold is exceeded a large percentage of the time in arid and semiarid regions where sandy soils prevail. Gibbens et al. (1983) found evidence of significant wind movement of soil at the Jornada Experimental Range in New Mexico. In two transition zones occupied by mesquite dunes and grasses, soil losses over the respective study areas of 4.6 cm (1933–1980) and 3.4 cm (1935–1980) were found. A third study area located entirely in the mesquite dunes experienced a net soil gain of 1.9 cm (1935–1980).

A number of studies have compared properties of dune and interdune areas. Hennessy et al. (1985) reported that dunes and interdunes differed greatly in soil particle size and surface temperature. Dune soils had much more sand and less silt and clay than interdune soils. Soil temperatures at depths of 30.5 cm and 122 cm were similar between bare interdunes and bare dunes, but soils of mesquite-covered dunes had considerably lower surface soil temperatures. Other physical variables such as bulk density, organic matter content, and electric conductivity were not much different in the two areas. Dunes did have greater infiltration but the interdunes had more soil water with depth and also experienced more evaporative losses. Greater infiltration in coppice dune soils as opposed to interdune soils was also found in studies in Nevada (Blackburn and Wood, 1990) and Idaho (Blackburn et al., 1990). Wright (1982) and Wright and Honea (1986) found greater total soil nitrogen beneath dunes than in interdunal areas. This was also reported by Whitford et al. (1995), along with greater infiltration, mineralization, and litter accumulation in dune areas. The presence of shrubs in desert grassland communities leads to the development of “islands of fertility” as a result of progressive cycling of plant nutrients confined to the zone beneath the shrubs. This leads to increased heterogeneity (Schlesinger et al., 1990). When the shrub involved is mesquite in a sandy region, coppice dunes can form, which not only affect the distribution of nutrients but also affect the aerodynamic roughness of the region. The potential for wind erosion is greater in the bare interdunes as opposed to the mesquite-covered dunes (Gould, 1982). Furthermore, the jetting effect around the edges of the scattered shrubs causes the wind velocity at the ground surface in the interdunes to be

greater than the average wind velocity in the open (Gould, 1982).

Similar coppice sand dunes (nebkas) are reported in areas of West Africa affected by desertification. Nebkas in Namibia range up to 3.5 m in height (Lancaster, 1995). The vegetation-topped dunes in Mali, which have developed in the last 30 years (Nickling and Wolfe, 1994), have lengths from 1.5 m to 17.9 m (average 5.45 m), widths from 0.9 m to 12.5 m (average 3.45 m) and heights from 0.35 m to 0.72 m (average 0.57 m). Coppice dunes have also been reported in Burkina Faso (Tenberg, 1995).

The study of sand dunes with remote sensing data in the southern High Plains and Southwest was started in 1928 when the first aerial photographs of the region revealed a type of dune never known to exist in this area (Melton, 1940). Melton (1940) classifies the shrub coppice dune as resulting from wind in conflict with clump vegetation (mesquite bush) in the absence of other effective sand binders such as grasses or thistle. Because mesquite grows vigorously on sand and is not readily killed by slow sand burial, a mound of sand is eventually built and held together by the coppice. In time, erosion on the windward side of the dune exposes the roots and kills the plant (Melton, 1940). The sand deposited on the lee side, however, furnishes suitable soil for the advancing mesquite. In this way, the dune sometimes slowly migrates with the wind, leaving a trail of dead mesquite wood. Melton (1940) indicated that these dunes may have a maximum height of 3 m and a maximum diameter of about 15 m. Melton (1940) also pointed out that a typical shrub coppice dune series was the precursor of greater sand concentration to come and the first topographic manifestation of increasing aridity.

METHODS

LIDAR Remote Sensing Data

A wide range of different types of remote sensing data have been collected at regular intervals over the part of the Jornada Experimental Range dominated by the coppice dunes. Until recently these data consisted of remote measurements made by passive instruments in the optical and thermal regions from the ground, air, and space. These imaging instruments are able to provide data at a range of spatial scales, and they allow the derivation of a number of important physical and semiempirical surface parameters; however, ordinarily they are unable to provide direct information on the physical structure of the surface at small scales (i.e., microtopography). For the calculation of aerodynamic roughness length and displacement height, it is necessary to have good estimates of the size, shape, and distribution of roughness elements, which in this case include both the dunes and the mesquite bushes that grow on them and are responsible for dune formation (Menenti and Ritchie, 1994; De Vries et al.,

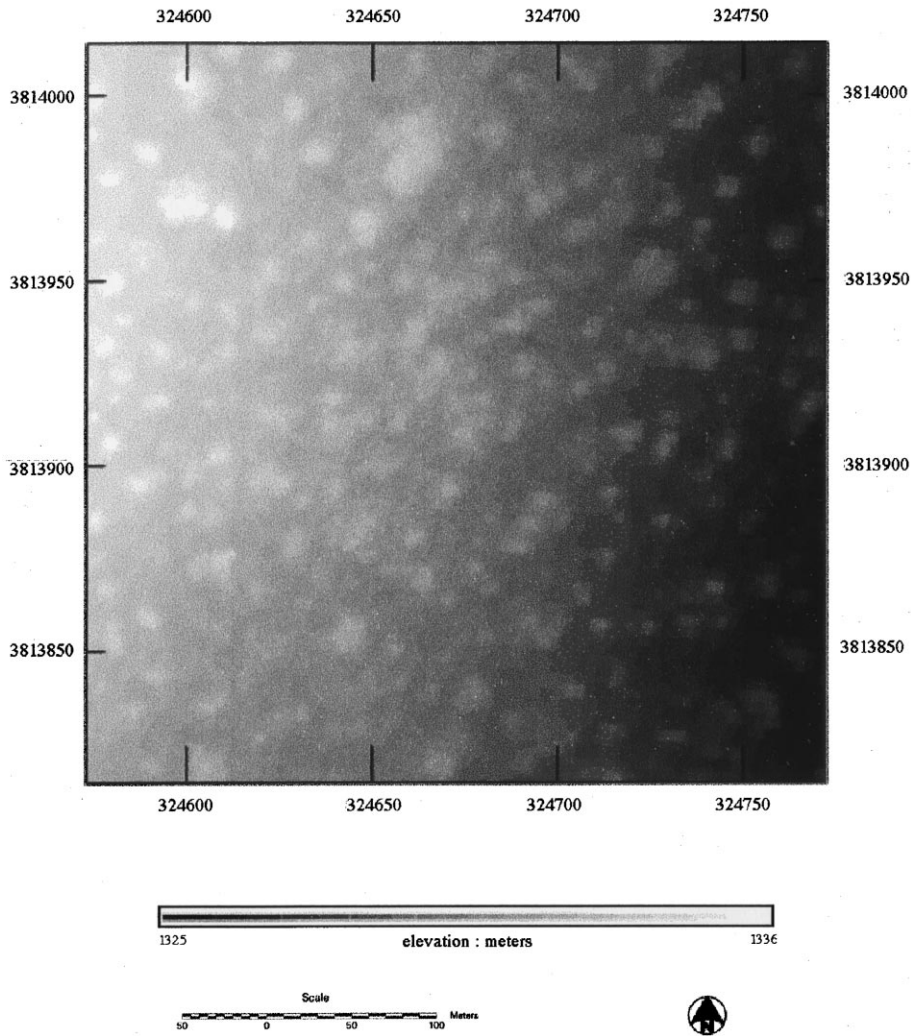


Figure 3. Digital Elevation Model (DEM) derived from scanning laser data over Mesquite Dune site, Jornada Experimental Range.

1999; De Vries, 1999). In recent years, active instruments that are able to provide accurate measurements of (relative) surface height at high resolutions have been introduced, notably profiling and scanning laser systems. These instruments are based on LIDAR (*L*ight *D*etection *A*nd *R*anging) principles; that is, they measure delays in the return signal from very short pulses of transmitted coherent light. Accurate location of laser returns is dependent on the use of differential global positioning systems and inertial navigation systems (DGPS and INS, respectively). Note that where the footprint is larger than features protruding from the surface (e.g., trees, shrubs) there may be multiple returns from laser pulses; in this case some systems allow simultaneous detection of objects and ground by separating these multiple returns. Recently, scanning LIDAR systems that allow measurement of the intensity of returns have been developed.

Airborne laser altimetry measurements (also known as profiling LIDAR) provide linear profiles of the relative heights of surface features. Data of this type were first acquired at the Jornada Experimental Range in May

1995 and have been made frequently since (Pachepsky and Ritchie, 1998; De Vries et al., 1999; De Vries, 1999). The data provided by this method are extremely precise in both vertical and horizontal planes with samples taken every 2 cm along the subflight path with a vertical resolution of 5 cm (Ritchie, 1995; Ritchie et al., 1996); the main disadvantages are that the areal dimensions of protrusions from the surface (dunes and mesquite bushes) must be estimated through statistical methods (i.e., by extrapolating from unidirectional measurements to two dimensions, making the assumption of no directional bias); and potential lack of stability in the horizontal plane as a result of undercorrection for the pitch, yaw, and roll movements of the aircraft. To match the profiling laser data to elevations extracted from the scanning laser digital elevation model (DEM), the former were subjected first to 24-point block averaging and then to spatial rescaling by least squares fits on the transect X or Y coordinates, depending on the direction of the flight.

Scanning laser data were acquired in February 1998 by Airborne Remote Mapping, Inc. (a subsidiary of Aero-

tec since March 1998), under contract to the USDA-ARS. The laser instrument was the Swedish Saab/TopEye system flown on a helicopter platform, using an across-track scanning system with a Z-shaped ground target path and with the along-track sampling rate determined by the speed of the aircraft. The wavelength of the laser is in the near-infrared at $1.064 \mu\text{m}$. The instrument operates in a number of modes, providing a sampling density adjustable from 1 to 15 samples per m^2 and with swath widths from 21 m to 168 m corresponding to minimum and maximum footprints of 0.06 m and 3.84 m. The laser pulses have a frequency of 7 Hz and up to five returns are recorded per sounding. The maximum scan angle is 20° , reducing but not entirely eliminating the impact of relief displacement, shadowing, and layover. The data used here were acquired in a low-density sampling mode and were supplied in files of X, Y, and Z values in the UTM reference system with an average sampling interval of about 2 m between footprints in the across-track direction (approximately east to west) and about 1.5 m in the along-track direction (approximately north to south). The footprint diameter was set at 0.38 m and the data were acquired in a single pass.

The study area was defined by a rectangular subset of 200×200 m centered over the coppice dune flux measurement site at $106^\circ 052.162' \text{W}$ by $32^\circ 039.039' \text{E}$ and the corresponding subset of points (XYZ records) was extracted. These points were used to construct a raster digital elevation model (DEM) with a cell size of 0.5 m in both X and Y by distance-weighted nearest-neighbor interpolation on the elevation values at three points (Fig. 3). Note that the scanning laser data include returns from the top of mesquite and other vegetation elements as well as from the soil surface. In spite of this, it is possible to produce a thematic map of dune boundaries from the DEM, which may be deemed reasonably accurate within certain limits. Two methods were initially pursued: thresholding on a slope image derived from the DEM and thresholding following progressive detrending of the DEM. Both methods have advantages and disadvantages, but the former is less attractive. Using a slope image to detect dunes edges is problematic since not all dunes have steep slopes defining their edges; moreover, extracting the edges to obtain discrete polygon features is difficult to automate. Progressive detrending has the advantage of being easily automated but also has disadvantages. It assumes that the trend in the interdune level remains relatively linear across the study area and is more prone to errors in interpolation, caused for example by the presence of mesquite on the tops of the dunes and (at the edges) by the lack of samples beyond the boundary of the study site.

Progressive detrending of the DEM has the effect of removing progressively smaller scales of variation in the data, beginning with the trend across the entire image. It can be effected by subtracting polynomial trend surfaces obtained at several levels. In this case, the large-

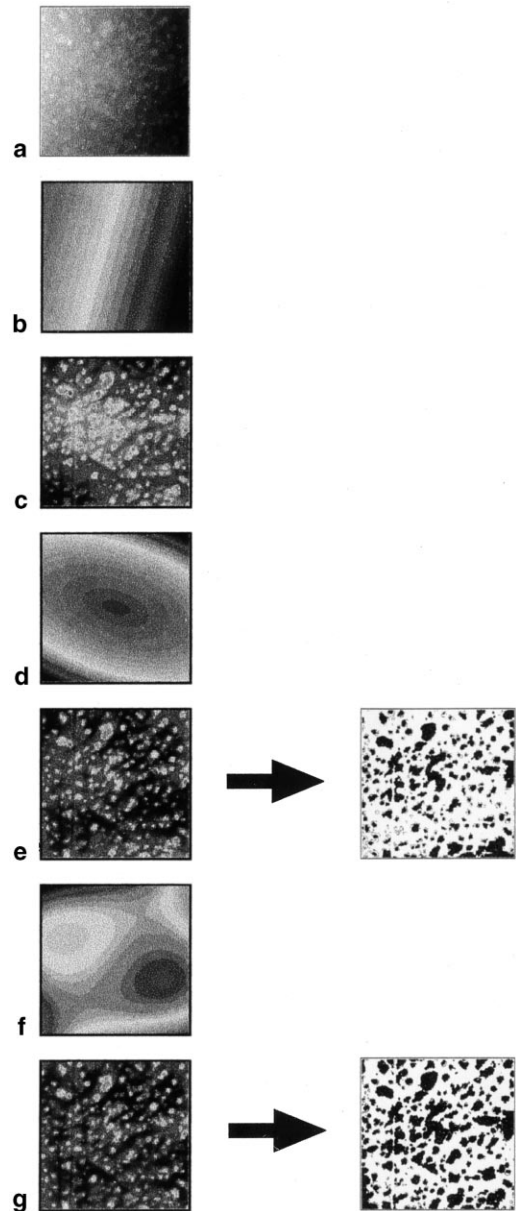


Figure 4. Construction of dune maps through progressive detrending of scanning laser digital elevation model.

scale slope rising from east to west was removed by subtracting a fitted linear surface and then the second degree curvature (northeast to southwest) was removed by subtracting a fitted quadratic surface. A third degree of curvature was removed to obtain a second detrended product by subtracting a cubic surface from the result of the previous detrending operations (see Fig. 4). Thresholds were then chosen based on the distribution of the values in the resulting file, the location of mesquite shrubs in coregistered digital video imagery (see below), and on the location of dune edges in the slope image. The two derived dune images are referred to as PD2 (*Progressive Detrending, 2 levels*) and PD3 (*Progressive Detrending,*

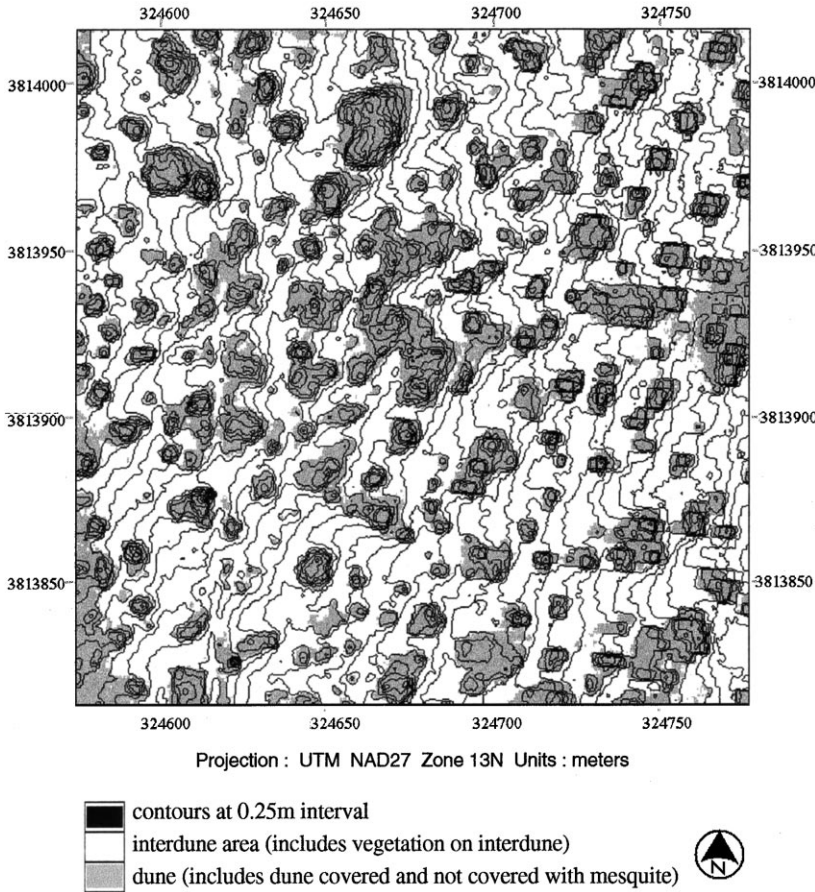


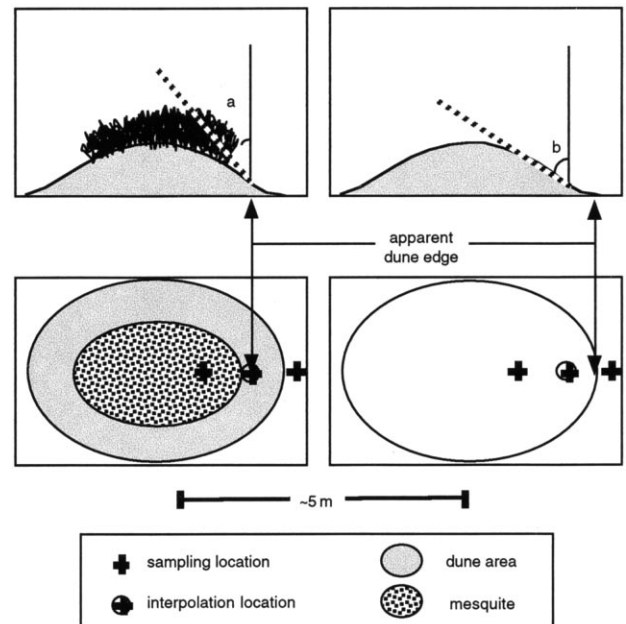
Figure 5. Mapped dunes with 0.25 m contours (PD3 method).

3 levels), respectively. The PD3 dune map is shown in Fig. 5, along with contours at 0.25-m intervals generated from the DEM. A third dune map was constructed by superimposing a filtered slope image derived from the original DEM over the PD2 image, which in this context is considered to provide the dune core areas. The slope image was subjected to 3×3 cell median filtering prior to overlay. The filtered slope image provides the dune edges, which do not appear in the PD2 images (Fig. 6), by selecting only the slopes greater than 9°. The combined map is further subjected to 3×3 cell maximum and 3×3 cell median filtering. This third dune map is referred to as PDS (*Progressive Detrending with Superposition of slope image*).

Reference Data

The data from the scanning laser may provide a useful means of acquiring information on surface morphology but require testing against some reference standard (i.e., validation). Here this is achieved directly and quantitatively with ground-based engineering survey transects and indirectly and qualitatively with digital multispectral video data in three bands: green (0.55 μm), red (0.65 μm), and near-infrared (0.85 μm). In addition, comparisons are made with linear profiling laser transects, although these data are less appropriate as reference data since they are

Figure 6. Potential shortening of distance from dune sill (dune top) to dune edge for a dune with mesquite (left), compared with a dune without mesquite (right); $a \ll b$. Top: side view; bottom: areal view.



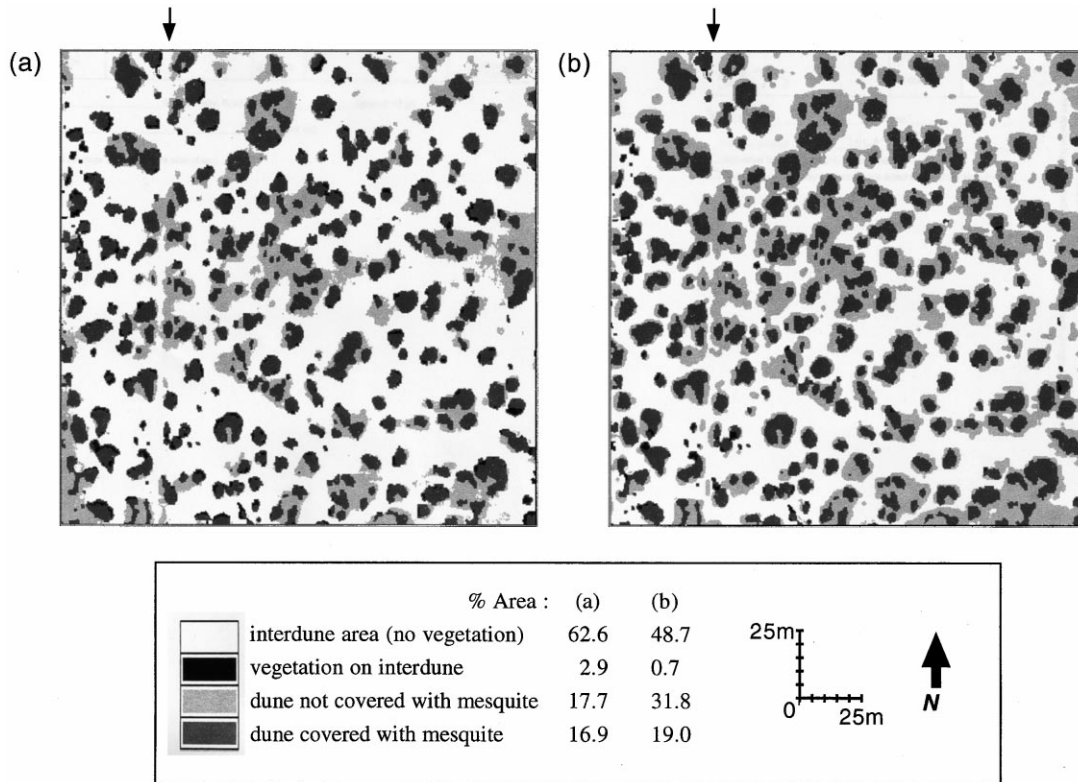


Figure 7. Spatial distribution and areal proportions of dunes and vegetation: (a) calculated via cross-classification of PD3 dune map and classified video; (b) calculated via cross-classification of PDS dune map and classified video. The arrows indicate the location of the north end of the road, which runs almost north-south.

more difficult to collocate with the other forms of data. The engineering surveys were carried out in June 1997 and comprise elevation measurements taken every 0.5 m along a 100-m transect in north/south, south/north, and east/west directions from a common starting point near the center of the study area. The measurements are based on established transit line-of-sight techniques and include the height of the soil surface and the mesquite bushes, where these occur.

The multispectral video image used was acquired on 16 February 1996 from an altitude of around 599 m above ground level (1,859 m above sea level). The image was registered to the DEM by a third-order polynomial transform using 15 evenly distributed control points derived from distinct features in both sets of images, providing a nominal root-mean-square error (RMSE) at the control points of 0.64 m in X, 0.91 m in Y, and 1.11 m in total. This error is low in relation to the resolution of the data. The video image has a ground resolution element (GRE) of ~ 0.64 m at this altitude, so there is a maximum shift of one cell in X. The data were acquired at about 2:20 P.M. LST when the solar zenith angle is low and so shadowing of the soil by mesquite or dunes is unlikely to present a significant problem in discriminating soil and vegetation. The video data were subse-

quently classified into soil and vegetation classes via RGB clustering with a one standard deviation limit in the three-space of the red, green, and near-infrared image planes. The spectral and brightness dissimilarities between the vegetation and the soil result in a broad classification that appears to be highly accurate (Everitt et al., 1997). In the resulting map the mesquite polygons had rather aliased (“stepped”) edges. The map was therefore cleaned by applying a 3×3 median filter. A small gap on the west side of the image (where the date, time, altitude, airspeed, and approximate location were stamped into the video) and representing less than one tenth of the image width was filled with classified video data from an earlier overflight in 1995. Note that the vegetation component includes sparse yucca on the interdune areas as well as honey mesquite on the coppice dunes themselves. The yucca are easily differentiated by their small size in relation to the mesquite shrubs and are not considered when calculating dune and vegetation statistics.

Testing Criteria

To test whether the scanning laser data are able to provide a model of the surface that is accurate for the purpose of determining dune morphology, the DEM data were compared to both sets of reference data. For a quan-

Table 1. Estimates of Dune and Mesquite Areas (for Study Area) from Detrended Scanning Laser and Digital Video Data

Area Calculation	PD3/Vegetation Map		PDS/Vegetation Map	
	m ²	%	m ²	%
Dune, no mesquite	14,160	17.7	25,360	31.7
Dune, with mesquite	13,520	16.9	15,200	19.0
Interdune, with mesquite	2,320	2.9	560	0.7
Interdune, no mesquite	50,000	62.5	38,880	48.6
Total	80,000	100.0	80,000	100.0

Dune/vegetation maps derived using three levels of detrending (PD3) and using two levels of detrending and filtered slope image (PDS).

titative comparison, the engineering survey transects and profiling laser overpass lines were located on the interpolated DEM and the corresponding raster samples were extracted. The DEM data were fitted to the engineering survey transects by least squares with little error ($r^2=0.96$). Note that there was no requirement to relocate the data (i.e., seek a spatial match) and only linear rescaling of the elevation values was necessary. This shows that the scanning laser data were geolocated with reasonable precision. The profiling laser data required linear (bias and offset) adjustment of the sample spatial coordinates (carried out visually) as well as the elevation values to obtain a match (i.e., both spatial and value rescaling was required). Location of the subflight line was aided by reference to analog video recordings that show the position of the profiler targets as the aircraft overflies the study area; however, obtaining a close match was found to be difficult.

A qualitative indication of the quality of the interpolated dune model derived from the scanning laser data is provided through comparison of the mapped locations of the mesquite shrubs (from registered digital video) and the coppice dunes. If the assumption is made that all mesquite occurs inside the boundaries of the dunes,

since the dunes are formed by entrapment of windblown soil materials by the mesquite (Lancaster, 1995; Zimmer, 1995), the thematic dune/mesquite cover map should show mesquite shrubs entirely enclosed by dune polygons. The comparison is made by cross-classification of two selected thematic dune maps PD3 and PDS (derived from the scanning laser DEM) with the vegetation-soil map (derived from classified video). The resulting raster images have four classes: dune with no mesquite, dune with mesquite, interdune with no mesquite, and interdune with mesquite.

The architecture of mesquite shrubs is such that even without leaves (e.g., burned) there is still an important woody element (Fig. 2). As a test of the feasibility of correcting for the effects of sampling over mesquite shrubs, a series of new DEMs were constructed. First, the mesquite boundary image was converted to a vector polygon coverage and an identity overlay operation was carried out with the original scanning laser data point coverage to produce a new point coverage with the attributes of both coverages. A formula was used to convert the original XYZ data in feet to meters for all points lying outside the mesquite polygons and to additionally subtract values of 0.1, 0.5, and 1.0 for all points lying inside

Table 2. Main Dune Statistics for Study Area from PD3 (detrending only) and PDS (detrending and slope)

	Dune Elevation		Dune Height ^b (m)	Area (m ²)	Perimeter (m)	Compactness Ratio
	Mean (m)	StDev ^a				
PD3						
min	1325.8	0.02	0.04	2.0	7.0	0.28
max	1335.3	0.76	4.02	1443.0	488.0	0.84
mean	1330.7	0.23	0.98	85.7	45.2	0.68
range	9.5	0.74	3.97	1441.0	481.0	0.56
stdevp	2.6	0.15	0.71	172.3	59.1	0.11
PDS						
min	1325.7	0.01	0.02	2.0	6.0	0.21
max	1334.9	0.87	4.80	3308.8	974.0	0.84
mean	1330.5	0.29	1.24	142.2	63.0	0.67
range	9.1	0.86	4.77	3306.8	968.0	0.63
stdevp	2.4	0.17	0.85	319.6	97.6	0.13

^a Population standard deviation.

^b Nominal height calculated as maximum elevation minus minimum elevation for each dune. Only dunes > 2 m² are considered. See text for derivation of compactness ratio statistic.

the mesquite polygons. These values were chosen as the average height of mesquite shrubs on the coppice dunes (~ 0.5 m) multiplied by various probabilities of a laser pulse over a shrub hitting an element at the top of the canopy rather than the lower parts of the canopy close to the soil, taken here as 0.1, 0.5, and 1.0. Interpolation was effected on the new XYZ data sets in the same manner as for the original data to produce new raster DEMs. Profiles from the original DEM and the three corrected DEMs corresponding to the north and south engineering survey transects were extracted and fitted to the survey data by least squares (without spatial rescaling).

Measures of Dune Morphology

Dune morphology may be quantified by a large number of metrics. Only the simplest are given here, including measures and distributions of dune and interdune area, dune perimeter length, dune height, and dune compactness. Note that dune height is calculated as a local dune height (i.e., the maximum elevation minus the minimum elevation) for each dune. The compactness ratio value for each of the dunes in the study area provides a measure of the degree to which an object's areal shape departs from that of a circle (Eastman, 1993). It is calculated as shown in Eq. (1):

$$C = 0.5 \sqrt{A_p/A_c} \quad (1)$$

where C is the compactness ratio, A_p is the area of the polygon for which a compactness ratio measure is required, and A_c is the area of a circle having the same perimeter as the candidate polygon. A value of unity indicates a shape close to circular while smaller values indicate more dendritic shapes.

RESULTS

Areal Cover Proportions of Dune, Interdune, and Mesquite

The two derived thematic cover maps are shown in Figure 7. From these the areal proportions of the four cover types may be calculated (Table 1). Dune areal extent differs considerably in the two maps. The total proportion of the study area accounted for by the dune class is 34.6% and 50.7% for the PD3-vegetation and PDS-vegetation maps, respectively. The correspondence between the location of the mesquite and dune classes is generally very good, with a more realistic representation of dune cover in the PDS-vegetation map. Here the boundaries of the dunes are generally more extensive than those of the mesquite shrubs. An area of dune slope outside the boundary of the mesquite would be expected since the sides of the dunes are never normal to the interdune surface. This has been confirmed by extensive field checks in the study area as part of JORNEX'99 (May–June). The important presence of a “vegetation on interdune” class in the PD3 cover

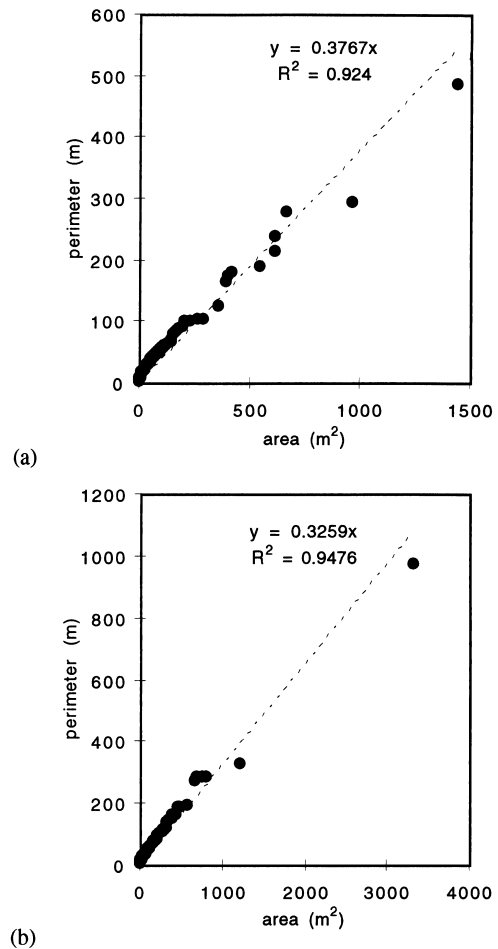


Figure 8. Dune area versus dune perimeter for (a) PD3 and (b) PDS methods.

map may be considered anomalous, since there should be no mesquite that does not grow on a dune. This class accounts for 2.9% of the total area. Although a small proportion of this can be attributed to yucca and snakeweed, most is a result of underestimation of dune extents. When the dune edges derived from the filtered slope image are superimposed on the dune core map to provide the PDS cover map, the occurrence of the “vegetation on interdune” class is reduced considerably to account for only 0.7% of the total area.

Dune Areas and Perimeters

In calculating per dune statistics a lower dune area limit of 2 m² is set to eliminate features that are not considered dunes. This results in mean dune area statistics of 85.7 m² and 142.2 m² for the PD3 and PDS dune maps, respectively, with mean perimeter lengths of 45.2 m and 63.0 m, respectively (Table 2). The mean statistic for the PDS map is strongly affected by an outlier (one very large dune of 3,309 m²), while the PD3 dune map has a maximum area of 1,443 m². If the outlier is not considered, the mean dune size for the PDS map is still 119.9

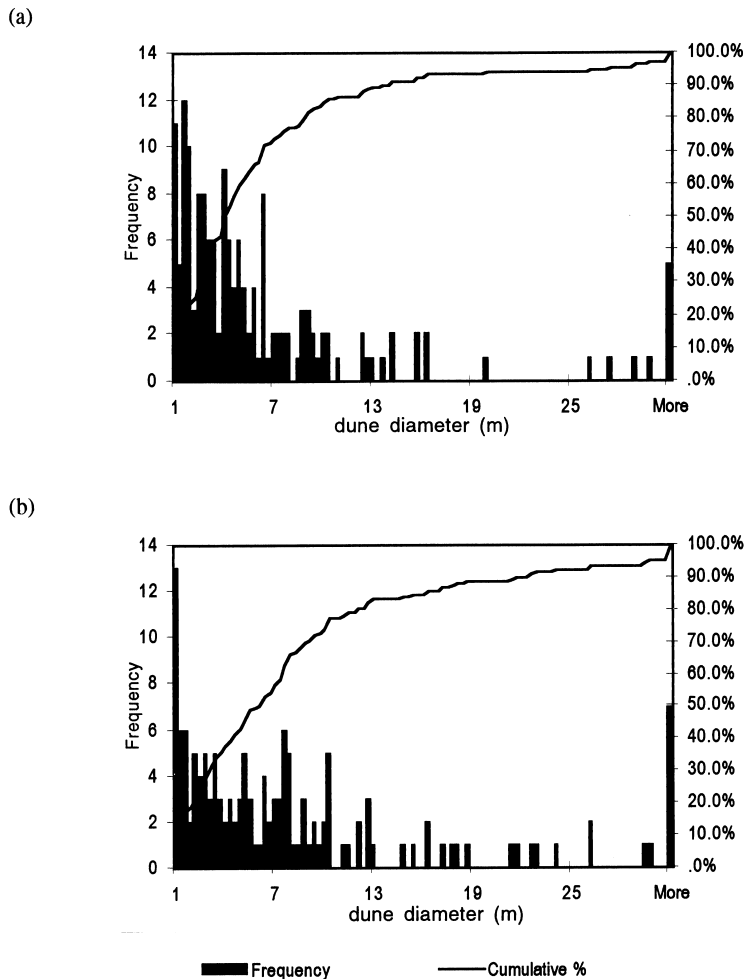


Figure 9. Frequency distributions for dune diameters (a) PD3 dune map; (b) PDS dune map (bin range based on 5% and 95% limits for the PDS distribution, which has the largest range of values).

m^2 . Figure 7 shows the difference in the areal distributions of dunes obtained via the PD3 and PDS methods; it can be seen that dunes in the PDS map are nearly always greater in extent than those in the PD3 map. The dune area frequency distributions provided by the two methods differ mainly in the number of large dunes, although below 400 m^2 there is a bimodal distribution with the distribution for PDS having a larger size for the second peak than PD3. The relationship of dune area to dune perimeter is surprisingly linear in both PD3 and PDS dune maps, although the mean perimeter:area ratio is lower for the latter (Fig. 8). Although there is no “correct” method to use (PD3 versus PDS), it is possible that the PD3 approach would be more appropriate in defining the islands of fertility of interest to ecologists and that the PDS approach would be more pertinent to micrometeorologists interested in the effects of roughness.

Dune Heights and Diameters

The distribution of nominal dune heights differs between the PD3 and PDS dune maps, with a smaller proportion of low dunes and a higher proportion of high dunes in the PDS map. Maximum dune height is greater when calcu-

lated using the PDS map than when using the PD3 map, with a wider range of heights, and mean dune height is 0.8 m greater (Table 2). Note that this is largely due to lower minimum dune elevations. Dune diameter is calculated as the diameter of a circle with the same perimeter as the actual dune. Note that this does not take the areal shape of the dune into account but avoids choosing a direction for measuring diameter. The frequency distributions of dune diameters are rather different for the PD3 and PDS maps, as expected, with a higher proportion of dunes with smaller diameters in the former (Fig. 9).

Dune Compactness

A negative exponential relationship appears to exist between dune size and dune compactness, with smaller dunes having simpler, more compact shapes and larger dunes having more complex, less compact shapes. This relationship holds true for the dune maps created using both the PD3 and PDS methods (Fig. 10). The frequency distribution of compactness ratio values on a per dune basis is skewed towards large values (>0.5), which is reasonable since the majority of dunes have a quasi-circular shape. Note that the different delineation meth-

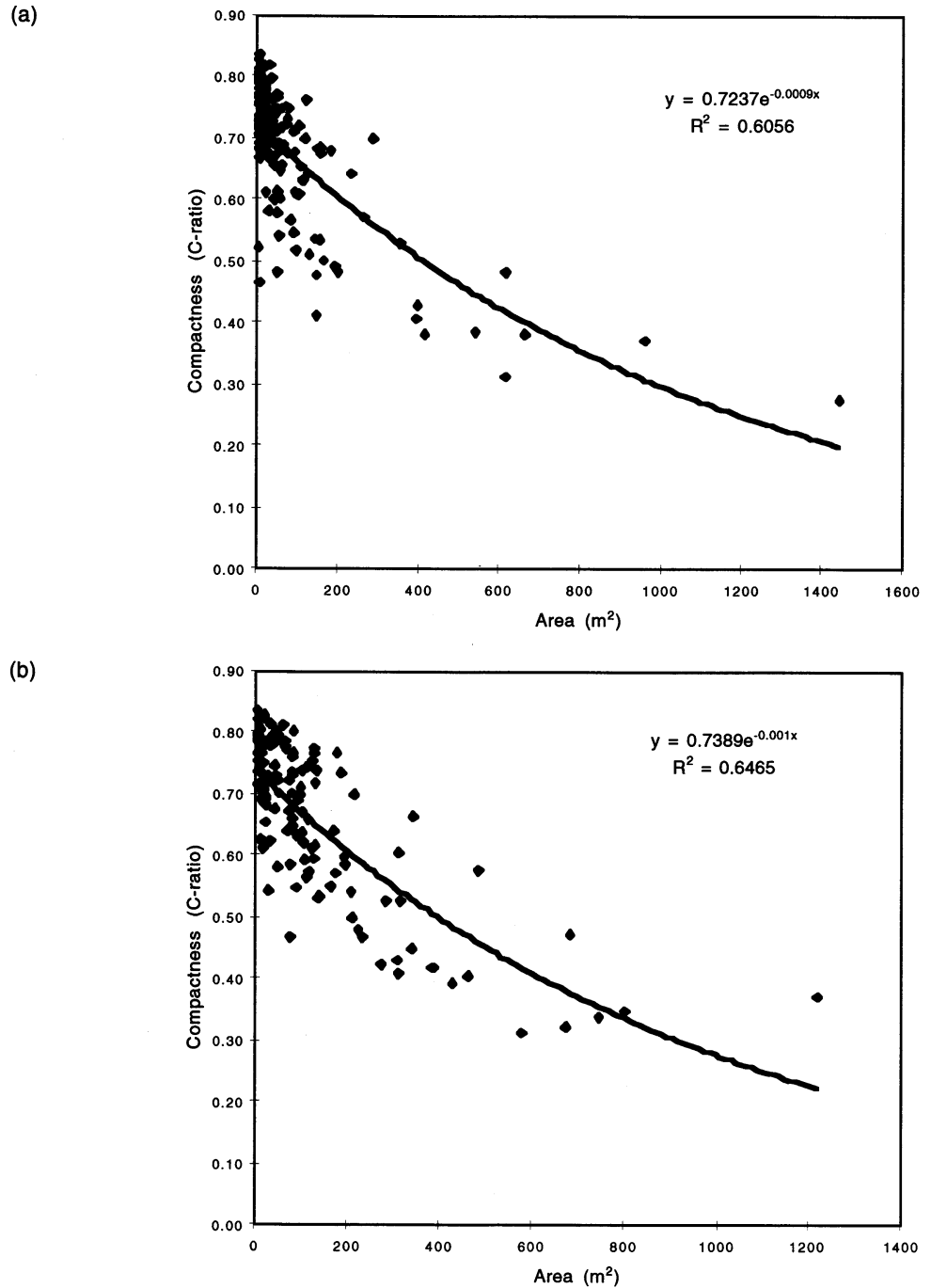


Figure 10. Relationship between dune area and dune compactness (excludes shrubs less than 2 m in diameter): (a) PD3 method, (b) PDS method (excluding a single large dune outlier).

ods also result in large differences in dune shape because the inclusion of dune edges from the slope image in PDS leads to the joining of dunes that were separate entities in the PD3 map (Fig. 7).

DEM Accuracy Testing

The validity of the measures of dune morphology given above is dependent on the ability of the scanning laser data to provide an accurate model of the topography of the mesquite coppice dune zone with a precision comparable to that provided by conventional engineering sur-

vey techniques. Figures 11 and 12 show profiles from the scanning laser image against those from the engineering survey transects for soil and soil+vegetation, together with the associated thematic and interpolated DEM data. The scanning laser profiles were adjusted against the engineering survey transects by least squares (linear transformation) and good matches were found with coefficients of determination (r^2) from 0.93 to 0.98.

Attempts were made to match profiles from transects acquired by the profiling laser to the DEM, although locational as well as value rescaling was required

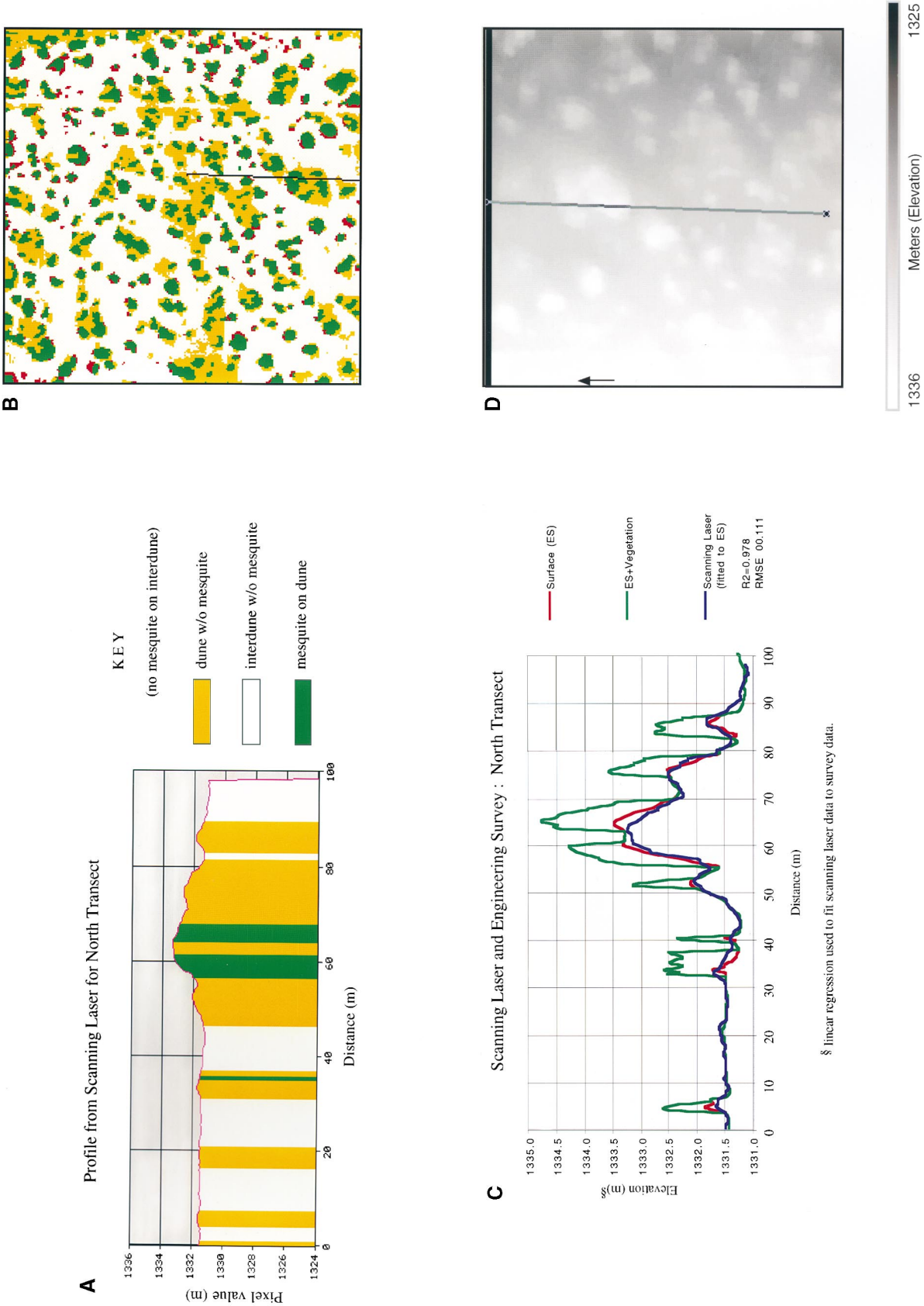
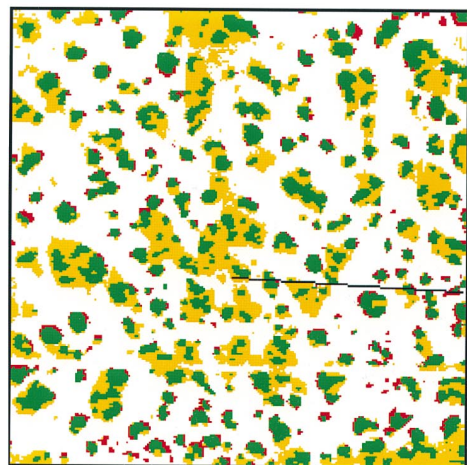
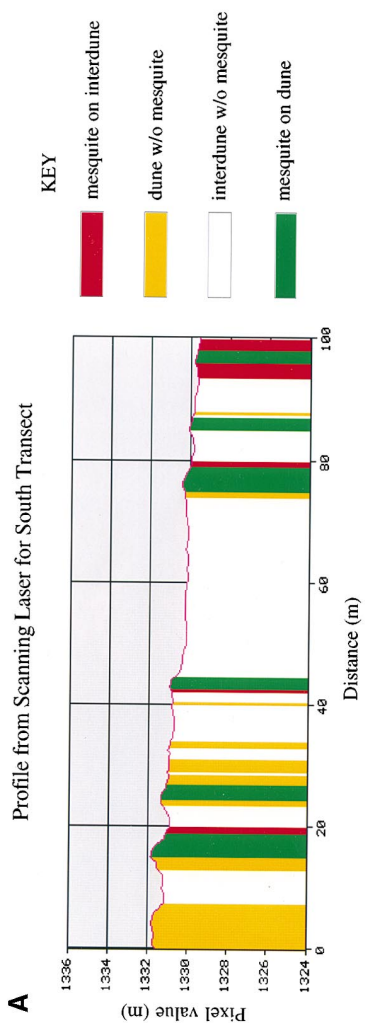


Figure 11. Vertical profiles from interpolated scanning laser DEM and engineering survey: north transect. (a) Scanning laser data profile showing occurrence of mesquite: Y-axis is Z-value; (b) engineering survey and laser-derived profiles; (c) thematic map from PD3 and video showing location of survey transect; (d) detail of DEM from interpolated scanning laser (arrow shows direction of sampling). The transect runs north for about 100 m from a point close to the center of the study area.



B

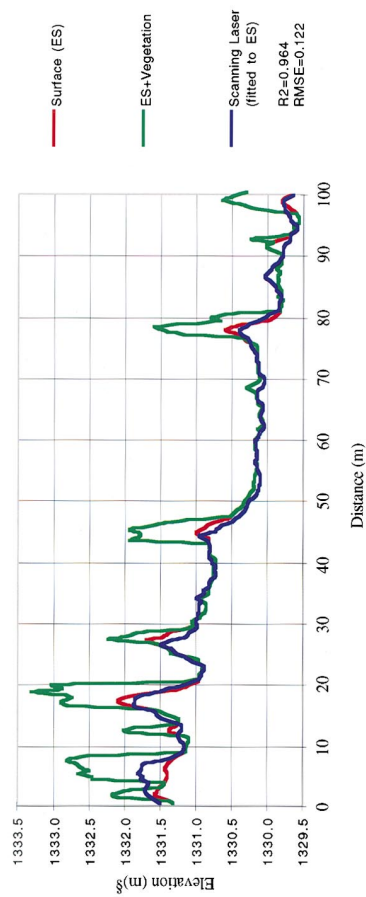


A



D

C Scanning Laser and Engineering Survey : South Transect



§ linear regression used to fit scanning laser data to survey data.



Figure 12. Vertical profiles from interpolated scanning laser DEM and engineering survey: south transect. (a) Scanning laser data profile showing occurrence of mesquite: Y-axis is Z-value; (b) engineering survey and laser-derived profiles; (c) thematic map from PD3 and video showing location of survey transect; (d) detail of DEM from interpolated scanning laser (arrow shows direction of sampling). The transect runs south for about 100 m from a point close to the center of the study area.

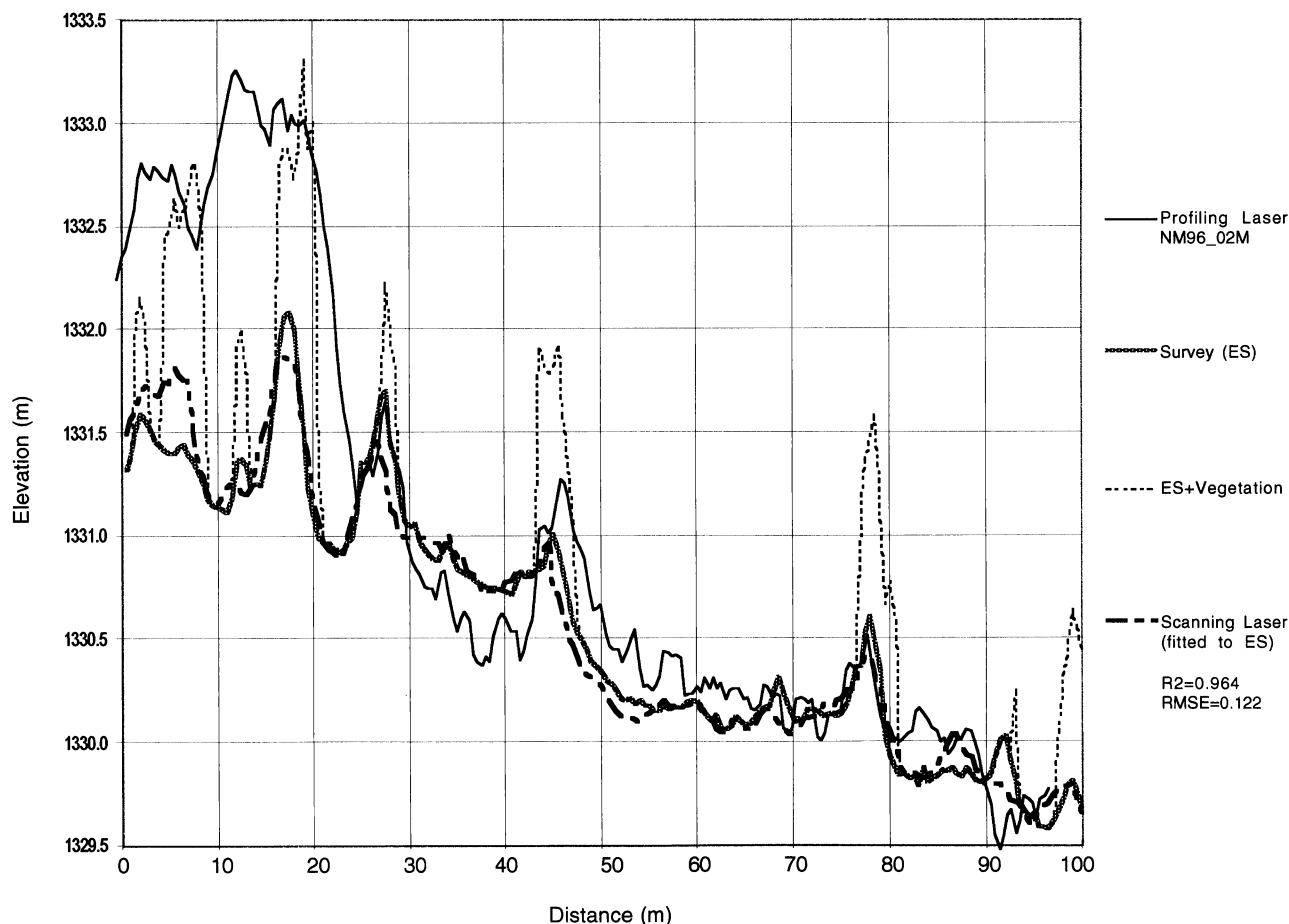


Figure 13. Best match of profiling laser to scanning laser DEM and engineering survey transit data (profiling laser data subjected to 24-point block averaging and spatial rescaling by slope and offset fit to scanning laser data).

and these attempts were not always entirely successful. In one case, a laser profile from February 1996 was successfully adjusted to match the corresponding data extracted from the scanning laser DEM. However, the results of other attempts were less conclusive but the difficulty of collocating the profiling laser data is the most likely explanation. Thus far it has only been possible to match a single profiling laser data transect to the ground engineering surveys, although this match is good with the subflight path diverging from the ground survey transect by less than 0.5 m normal to the latter in any direction. A comparison between the corresponding (rescaled) pro-

filed laser, extracted scanning laser, and engineering survey elevation data is shown in Figure 13.

The results of assuming a proportion of returns from mesquite shrub elements rather than dune top soil surfaces show that the profiles corrected for the effects of sampling over mesquite exhibit weaker relationships to the engineering survey profiles than to the original DEM (Table 3), although it can also be seen that in some instances the profiles from the corrected DEMs provide a slightly better local match (Fig. 14).

DISCUSSION

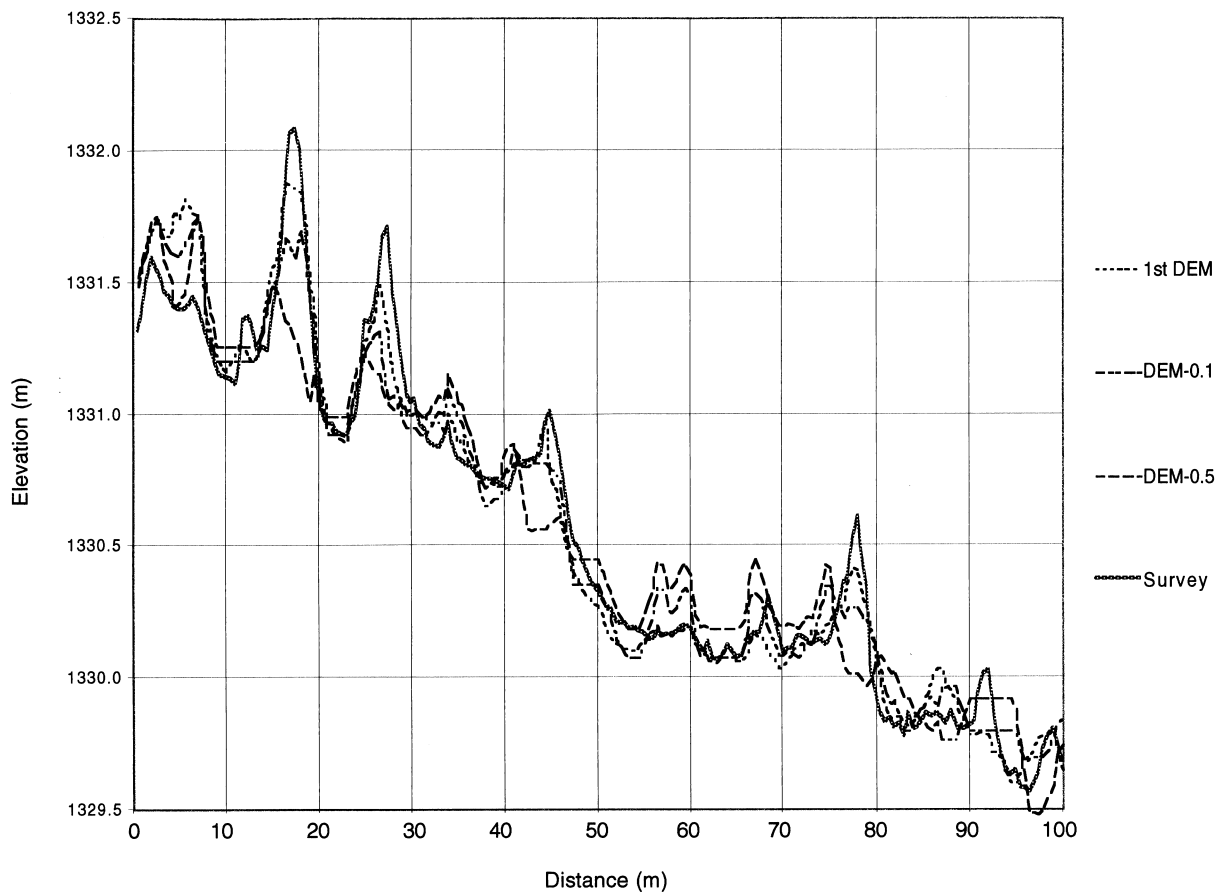
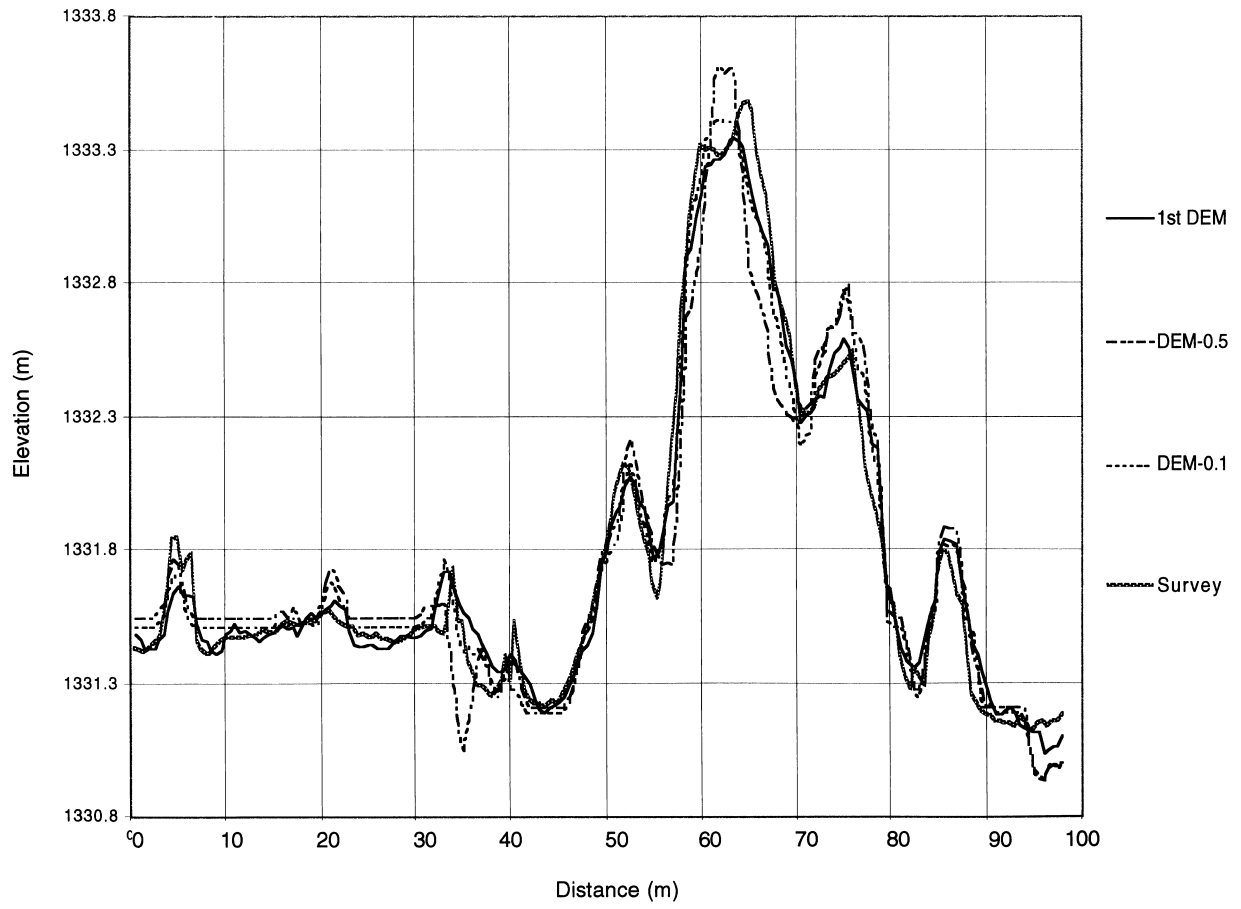
The combination of the classified video data with the mapped dunes in a thematic map shows that in general

Table 3. Strength of Relationships (R2) between North and South Engineering Survey Profiles and Those Obtained from Scanning Laser (Both With and Without Correction of Interpolated DEM for the Presence of Mesquite)

Deduction (m)	N Transect	S Transect
0.00	0.98	0.96
0.10	0.96	0.95
0.50	0.91	0.88
1.00	0.70	na

na=not available.

Figure 14. Profiles from original scanning laser DEM (1st DEM); DEM with 0.5 subtracted over mesquite (DEM-0.5); DEM with 0.1 subtracted over mesquite (DEM-0.1); and engineering survey transit data (Survey). (a) North transect; (b) south transect. The transects run north and south, respectively, for about 100 m from a point close to the center of the study area.



the dune polygons do enclose the mesquite polygons (Fig. 7). In the first dune map constructed (PD2; not shown) sliver polygons of the “vegetation on interdune” class were very apparent at the peripheries of many of the mapped dunes and overall accounted for an important proportion of the total area (~11%). This proportion was reduced to under 3% by a further level of detrending (PD3), although it should be negligible in the case where accurate models of the dune and vegetation distributions are obtained. The presence of this class is deemed to be due to one or several of the following factors:

- The mesquite shrubs are actually growing outside the boundaries of the dunes.
- The classification is inaccurate and the “mesquite” class includes much shadow.
- There are large registration errors between the vegetation and dune maps.
- The airborne video data are adversely affected by the phenomenon of relief displacement.
- Error exists in the estimation of dune areal extent (i.e., error in the data used in interpolation plus interpolation error, plus error owing to the detrending and choice of thresholds).
- The locations of the mesquite shrubs and/or the dunes changed in the 24 months elapsing between the acquisitions of the two data sets.

The first and second factors are not thought likely to be important for the reasons already mentioned. Registration error is unlikely to be uniquely responsible since this is less than 0.5 m in both X and Y directions and there is no consistent directional bias in the distribution of the “vegetation on interdune” class polygons (this also precludes important shadowing effects). It is also unlikely that the locations of the dunes would have changed over the 24-month period. According to Gibbens et al. (1983), of the 65 dunes persisting in 1980 at a transect originally sampled in 1935, the mean movements by direction were 1.95 m west, 2.35 m east, 3.75 m south, and 3.84 m north. Those dunes moving the most rapidly (in a northerly direction) therefore did so at an average rate of 8.53 cm yr⁻¹. Applying this to the current study area, in the absence of exceptional conditions the dunes could have moved by about 21 cm, not enough to account for the observed anomalies in the PD2 and PD3 maps. However, note that severe short-term events may mean that the average rate is not always a reliable measure.

The problem seems more likely to be due to a combination of errors in the estimation of dune areal extent and relief displacement effects, which are difficult to quantify. The interpolation of the DEM from sparsely sampled points is likely to lead to poor elevation estimates where there is a change in the actual elevation at a smaller scale than that resolvable by the laser system. Critical to the estimation of dune areal extent using these methods, interpolation on rather spatially coarse eleva-

tion data leads to a high probability of sometimes including returns from the tops of mesquite shrubs close to the dune sill (edge of the flattened dune top), resulting in a steeper apparent slope from the edge of the top of the dune to the surrounding interdune area and thus shortening the apparent distance from the dune sill to the dune edge (Fig. 6). Although it may appear unlikely that this problem can be overcome without a more dense sampling regime, two alternative approaches can be considered. The first is to use progressive detrending of the interpolated DEM to obtain dune cores and a slope map to obtain the dune sides, as effected here to obtain the PDS dune map. The second is to make an adjustment for the additional height of the mesquite above the dune, wherever mesquite is apparent on video imagery. This requires that two further assumptions be made: (1) mesquite shrub height is constant (or can be estimated from other sources) and (2) every return within a mesquite polygon is actually from the top of the shrub and not from lower in the canopy or at the sill surface.

The results of tests of the feasibility of correcting for the effects of sampling over the mesquite shrubs indicate that the probability of returns from the top of the mesquite shrubs is quite low (less than 10%). This is partly because at the time of year that the scanning laser data were acquired (February) the shrubs are still dormant and without leaves (Fig. 2).

With respect to dune shape, smaller dunes were shown to have simpler, more compact shapes, and larger dunes had more complex, less compact shapes. Although there will be a small bias in area and perimeter calculations owing to the nature of the raster data model, this may indicate that dune shape changes in a consistent manner with time: as the dunes become larger they may join together to form more dendritic shapes (note that this assumes that deposition is a more important process than erosion).

CONCLUSIONS

The potential of moderate sampling density (1 m to 2 m between footprints) by scanning laser technology as a means for providing models of dune morphology over small areas has been investigated and appears to be viable, with good matches between a DEM from simple three-point interpolation and transit data from engineering surveys. The study has also shown that a major limit on accuracy for the case of a mesquite dune shrub land (i.e., the possibility of returns from dune and the tops of mesquite branches or both) is not a barrier to generation of a reasonably accurate model from which dune morphology and the arrangement of dunes in the landscape may be assessed, at least when data are acquired during the winter season when the shrubs are leafless and the probability of shrub top returns is low. Similar studies are now required using data acquired at

the peak of the growing season to investigate the impact of relatively dense mesquite canopies on LIDAR returns. Differences may also be useful in determining canopy structural measures such as canopy height, leaf area index, and leaf angle distribution. A recent study by Means et al. (1999) over forest stands in the Western Cascades of Oregon showed that large-footprint scanning LIDAR is capable of predicting canopy height, tree basal area, total biomass, and leaf biomass. These workers used the SLICER instrument with a swath consisting of only five measurements with a nominal 10-m diameter footprint, while the footprint of the TopEye system used here is more than an order of magnitude smaller (0.38 m).

The major limitations of scanning LIDAR are the reliance on the onboard differential GPS and INS systems and occasional difficulties with matching multiple scans. LIDAR distance measurements may provide very high relative precision but varying accuracy vis-à-vis some absolute measure of elevation above a given datum, and positional accuracy is difficult to determine. Foreshortening and shadowing are only likely to present a problem if the scanning angle is too high, for example in the case of high-density acquisitions by flying at very low altitudes. A high-density scanning LIDAR data set over the mesquite dune site from the TopEye system used here showed serious elevation anomalies at locations where two scans overlapped. Areal coverage is becoming less of a problem since new systems are emerging with swath widths of up to 1000 m and the capability to survey 1,000 km² (~385 square miles) in just 12 hours. Currently the maximum rate of operation is around 50 km² per hour. Until fairly recently, applications making use of scanning laser altimetry have been mostly limited to narrow corridor-type feature mapping and these applications continue to be important (an example is the mapping of coastal erosion, cf. National Oceanic and Atmospheric Administration, 1999). However, the rapid increases in computer processing speeds and inexpensive digital storage together with improved DGPS/INS integration are enabling applications over larger areas, which were hitherto difficult or impossible.

This study has shown that the combined laser-video capability can be used to measure the morphological characteristics of shrub coppice dunes in the desert grasslands of southern New Mexico with acceptable accuracy and precision for a range of uses, including important hydrological, biophysical, and aerodynamic applications that would otherwise require time-consuming ground-based measurement. To characterize both the areal and the vertical variability of these dunelands it is necessary to use distance measures from scanning laser in conjunction with classification measures from some other type of sensor, such as multispectral aerial videography or airborne electro-optical scanners. The use of such systems together is highly synergistic. In the future, new implementations will

provide a means of quantitatively mapping these islands of fertility and their islands of roughness over large areas.

The scanning laser data were provided to ARS by Aerotec under contract #53-3K47-5-011. We would like to thank the ARS Remote Sensing Research Lab., Weslaco, Texas, for providing video coverage of the test sites. Special thanks are extended to Mr. Rene Davis (ARS Weslaco) for flying the test sites as many times as needed, Mr. Jim Lenz and Mr. David Thatcher (ARS Jornada) for conducting the engineering surveys, and Ms. Koli Leach (ARS Beltsville) for data processing. Additionally, the outstanding field support at the Jornada Experimental Range has contributed to the success of this project. Finally the reviewers are thanked for their helpful comments and suggestions.

REFERENCES

- Archer, S. (1989), Have southern Texas savannas been converted to woodlands in recent history? *American Naturalist* 134(4):545–561.
- Archer, S. (1994), Woody plant encroachment into southwestern grasslands and savannas: rates, patterns and proximate causes. In *Ecological Implications of Livestock Herbivory in the West* (M. Vavra, W. Laycock, and R. Pieper, Eds.), Society of Range Management, Denver, CO, pp. 13–68.
- Archer, S., Scifres, C., Bassham, C., and Maggio, R. (1988), Autogenic succession in a subtropical savanna: conversion of grassland to thorn woodland. *Ecological Monographs* 58(2): 111–127.
- Bahre, C. J. (1991), *A Legacy of Change*. The University of Arizona Press, Tucson, Arizona.
- Belnap, J., and Gillette, D. A. (2000), Disturbance of biological soil crusts: Impacts on potential wind erodibility of sandy desert soils in SE Utah, USA. *Land Degradation and Development* 8(4):355–362.
- Blackburn, W. H., Pierson, F. B., and Seyfried, M. S. (1990), Spatial and temporal influence of soil frost on infiltration and erosion of sagebrush rangelands. *Water Resources Bulletin* 26(6):991–997.
- Blackburn, W. H., and Wood, M. K. (1990), Influence of soil frost on infiltration on shrub coppice dune and dune interspace soils in southern Nevada. *Great Basin Naturalist* 50(1):41–46.
- Buffington, L. C., and Herbel, C. H. (1965), Vegetational changes on a semidesert grassland range from 1858 to 1963. *Ecological Monographs* 35(2):139–164.
- De Vries, A. C. (1999), *Land Surface Roughness and Remote Sensing*, Doctoral Thesis, published by Rijksuniversiteit Groningen, The Netherlands.
- De Vries, A. C., Ritchie, J. C., Klaassen, W., Menenti, M., Kustas, W. P., Rango, A., and Prueger, J. H. (1999), Effective aerodynamic roughness estimated from airborne laser altimeter measurements of surface features. *Int. J. Remote Sensing*, in press.
- Eastman, J. R. (1993), *Idrisi Technical Reference Manual Version 4.0 Rev. 3 October 1993*, Clark University Graduate School of Geography, Worcester, MA, USA.
- Everitt, J. H., Alaniz, M. A., Davis, M. R., Escobar, D. E., Havstad, K. M., and Ritchie, J. C. (1997), Light reflectance characteristics and video remote sensing of two range sites on the Jornada Experimental Range. In *16th Biennial Work-*

- shop on Videography and Color Photography in Resource Assessment (Proceedings), Weslaco, Texas, April 29–May 1, 1997, pp. 485–495.
- Fredrickson, E., Havstad, K. M., Estell, R., and Hyder, P. (1997), Perspectives on desertification: South-western United States. *J. Arid Environments* 39:191–207.
- Gay, C. W., and Dwyer, D. D. (1998), *New Mexico Range Plants*, Cooperative Extension Service Circular 374, New Mexico State University, Las Cruces, NM, USA.
- Gibbens, R. P., Tromble, J. M., Hennessy, J. T., and Cardenas, M. (1983), Soil movement in mesquite dunelands and former grasslands of southern New Mexico from 1933 to 1980. *J. Range Management* 36(2):145–148.
- Gould, W. L. (1982), Wind erosion curtailed by controlling mesquite. *J. Range Management* 35(5):563–566.
- Grover, H. D., and Musick, H. B. (1990), Shrubland encroachment in southern New Mexico, USA: An analysis of desertification processes in the American Southwest. *Climatic Change* 17:305–330.
- Hastings, J. R., and Turner, R. M. (1965), *The Changing Mile*. The University of Arizona Press, Tucson, AZ, USA.
- Hennessy, J. T., Gibbens, R. P., Tromble, J. M., and Cardenas, M. (1985), Mesquite (*Prosopis glandulosa* Torr.) Dunes and interdunes in southern New Mexico: A study of soil properties and soil water relations. *J. Arid Environments* 9:27–38.
- Huenneke, L. F. (1996), Shrublands and grasslands of the Jornada Long-Term Ecological Research Site: Desertification and plant community structure in the northern Chihuahuan desert. In *Proceedings: Shrubland Ecosystem Dynamics in a Changing Environment* (J. R. Barrow, E. MacArthur, S. Durant, E. Ronald, R. J. Tausch, comps), May 23–25, Las Cruces, NM, General Technical Report INT-GTR-338, Ogden, UT: USDA, Forest Service, Intermountain Research Station, pp. 48–50.
- Lancaster, N. (1995), *Geomorphology of Desert Sand Dunes*. Routledge, New York, USA.
- Link, S. O., Waugh, W. J., Downs, J. L., Thiede, M. E., Chatters, J. C., and Gee, G. W. (1994), Effects of coppice dune topography and vegetation on soil water dynamics in a cold-desert ecosystem. *J. Arid Environments* 27:265–278.
- Martcorena, B., Bergametti, G., Gillette, D., and Belnap, J. (1997), Factors controlling threshold friction velocity in semiarid and arid areas of the United States. *J. Geophys. Res.* 102(D19):23277–23287.
- Means, J. E., Acker, S. A., Harding, D. J., Blair, J. B., Lefsky, M. A., Cohen, W. B., Harmon, M. E., and McKee, W. A. (1999), Use of large-footprint scanning airborne LIDAR to estimate forest stand characteristics in the Western Cascades of Oregon. *Remote Sens. Environ.* 67:298–308.
- Melton, F. A. (1940), A tentative classification of sand dunes: Its application to dune history in the southern high plains. *J. Geology* 48:113–145.
- Menenti, M., and Ritchie, J. C. (1994), Estimation of effective aerodynamic roughness of Walnut Gulch watershed with laser altimeter measurements. *Water Resources Research* 30(5):1329–1337.
- National Oceanic and Atmospheric Administration (1999), *Laser Beach Mapping*, NOAA Coastal Services Center, <http://www.csc.noaa.gov/text/beach.html> (latest access 8/12/99).
- Nickling, W. G., and Wolfe, S. A. (1994), The morphology and origin of Nabkhas, Region of Mopti, Mali, West Africa. *J. Arid Environments* 28:13–30.
- Pachepsky, Y. A., and Ritchie, J. C. (1998), Seasonal changes in fractal landscape surface roughness estimated from airborne laser altimetry data. *Int. J. Remote Sens.* 19(13):2509–2516.
- Rango, A., Ritchie, J. C., Kustas, W. P., Schmutge, T. J., and Havstad, K. M. (1998), JORNEX: Remote sensing to quantify long-term vegetation change and hydrological fluxes in an arid rangeland environment. In *Hydrology in a Changing Environment* (H. Wheatler and C. Kirby, eds.), John Wiley, London, pp. 585–590.
- Ritchie, J. C. (1995), Airborne laser measurements of landscape topography. *Rem. Sens. Environ.* 53:91–96.
- Ritchie, J. C., Rango, A., Kustas, W. P., Schmutge, T. J., Brubaker, K., Zhan, X., Havstad, K. M., Nolen, B., Prueger, J. H., Everitt, J. H., Davis, M. R., Schiebe, F. R., Ross, J. D., Humes, K. S., Hipps, L. E., Ramalingam, K., Menenti, M., Bastiaanssen, W. G. M., and Pelgrum, H. (1996), JORNEX: An airborne campaign to quantify rangeland vegetation change and plant community—atmospheric interactions. In *Proceedings of the Second International Airborne Remote Sensing Conference and Exposition, Technology, Measurement and Analysis*, Vol. II, San Francisco, California, pp. 54–66.
- Schlesinger, W. H., Reynolds, J. F., Cunningham, G. L., Huenneke, L. F., Jarrell, W. M., Virginia, R. A., and Whitford, W. G. (1990), Biological feedbacks in global desertification. *Science* 247:1043–1048.
- Smith, J. G. (1899), *Grazing Problems in the Southwest and How to Meet Them*. United States Department of Agriculture Div. Agros., Bulletin 16.
- Tenberg, A. (1995), Nebkha dunes as indicators of wind erosion and land degradation in the Sahel zone of Burkina Faso. *J. Arid Environments* 30:265–282.
- Valentine, K. A. (1942), Mesquite sandhills artificial revegetation experiments, 1934 to 1936. Unpublished manuscript, Jornada Experimental Range, Southwestern Forest and Range Experiment Station, Las Cruces, NM.
- Webb, R. H. (1996), *Grand Canyon, A Century of Change*. The University of Arizona Press, Tucson, Arizona.
- Whitford, W. G., Martinez-Turanas, G., and Martinez-Meza, E. (1995), Persistence of desertified ecosystems: explanations and implications. *Environmental Monitoring and Assessment* 37:319–332.
- Wooten, E. O. (1908), *The Range Problem in New Mexico*. New Mexico Agricultural Experimental Station Bulletin No. 66, Las Cruces, NM.
- Wright, R. A. (1982), Aspects of desertification in *Prosopis* dunelands of southern New Mexico. *J. Arid Environments* 5:277–284.
- Wright, R. A., and Honea, J. H. (1986), Aspects of desertification in southern New Mexico, USA: Soil properties of a mesquite duneland and a former grassland. *J. Arid Environments* 11:139–145.
- Zimmer, C. (1995), How to make a desert. *Discover* February.